Probabilistic seismic hazard assessment of district headquarters of Kashmir Valley in Jammu and Kashmir, India

Fida Anjum

Department of Civil Engineering,
Islamic University of Science and Technology,
Awantipora, Pulwama, 192122, Jammu and Kashmir, India
Email: fidaanjum65@gmail.com

Shaista Jan

Hindustan Petroleum Corporation Limited (HPCL),
Pampore, Pulwama, 192121, Jammu and Kashmir, India
Email: saimashaista07april@rediffmail.com

Yawar Mushtaq Raina*

Public Works (R&B) Department,
Division Rajouri, 185131,
Government of Jammu and Kashmir, India
Email: yawarraina35@gmail.com
*Corresponding author

Abstract: This study aims at characterising the probable 99 faults of region by carrying out the probabilistic seismic hazard analysis for different districts of Kashmir valley by preparing seismic hazard curves and the contour maps of three ground motion parameters, namely, peak ground acceleration (PGA), short period *Sa* (0.02 *s*) and long period *Sa* (1.0 *s*) spectral acceleration for 50, 100, 500 and 2,500 years return periods using the Atkinson and Boore (2006) GMPM and an updated catalogue containing event records till April 2018. On comparison with the earlier studies it was found that there is the need to consider the local site variability in the hazard computation. Shopian, Budgam, Baramulla and Kupwara were found to have much higher seismic hazard levels as compare to other districts. The estimated hazard values for these regions highlights that the zonal spectral values are underestimated in the Indian Codal provisions. The maps, hazard curves and UHRS so developed can be used for assessing the seismic vulnerability of the existing structures and constructing risk maps for the selected areas.

Keywords: seismicity; earthquake; Kashmir Valley; faults; contour maps; Himalaya; rocks; peak ground acceleration; PGA; short period; long period; spectral acceleration; India.

Biographical notes: Fida Anjum is working as an Assistant Professor in Department of Civil Engineering in Islamic University of Science and Technology Awantipora, J&K. She completed her Bachelors in Civil Engineering from Baba Ghulam Shah Badshah University Rajouri in the year 2015 and Masters in Structural Engineering from Sharda University in 2017. Her research interests include structural engineering, concrete technology, earthquake and environmental engineering

Shaista Jan is working as an operation officer in HPCL Bottling Plant in Pampore, Pulwama (J&K). She obtained her Bachelors in Civil Engineering form NIT Srinagar. Her research interests include study of rocks, geotechnical and earthquake engineering.

Yawar Mushtaq Raina is currently working as Junior Engineer in Public Works (R&B) Department Division Rajouri. He has also worked as Lecturer in Baba Ghulam Shah Badshah University for two and half years. He obtained his Bachelors in Civil Engineering from Baba Ghulam Shah Badshah University in 2012. His areas of interests include water quality and wastewater analysis, ground water hydrology, analysis and design of concrete structures.

1   Introduction

Probabilistic seismic hazard assessment (PSHA) is a technique of finding the prospect that different intensities of earthquake caused ground motions will be surpassed at a known place in future time period (Baker, 2008) The consequences of such an analysis are conveyed as predictable likelihoods per year. The improbability is considered as explicitly and annual prospect of surpassing specified ground motions is estimated. The main thing in stating seismic hazards is to identify seismic sources, lithology of an area, geomorphology, nature of soil and rocks, condition of groundwater table, building construction methods and kinds of set-up that could affect specific site at which is the study area (Chandra et al., 2018; Zafarani et al., 2017). These are called seismotectonic sources which forms the main part of investigation. Over the past decade it has been noted that Himalaya which is a 2,500 km long belt of mountains formed as a result of the progressive under thrusting of the Indian Plate beneath Tibetan Plate along Main Himalayan Thrust (MHT) and which Kashmir region is part of has been prone to frequent seismic activities. Global positioning system (GPS) measurements indicate 4–5 cm/year of convergence rate between these two plates of which 18 mm/year is accommodated by thrust systems along the Himalayan arc (Banerjee and Bürgmann, 2002).

Based on the active fault topography, the Main Boundary Thrust (MBT) and Himalayan Frontal Thrust (HFT) are considered as active (Nakata, 1989; Valdiya, 1980; Malik and Mohanty, 2007). As a result of this active fault and frequent seismic activities great loss to infrastructure and human life in general have been reported. The incidents of Kangra (1905), Kashmir (2005), Sikkim (2011) and Nepal (2015) are glowing instances of the earthquakes of the recent past in the whole Himalayan region (Ambraseys and Bilham, 2000; Kaneda et al., 2008; Rajendran et al., 2015; Mitra et al., 2015). More than 20,000 people during Kangra Earthquake (4 April 1905, Mw 7.8), 80,000 people during Kashmir Earthquake (8 October 2005, Mw 7.6), 115 people during Sikkim Earthquake (18 September 2011, Mw 6.9) and 9,000 people in Nepal Earthquake (25 April 2015,

Mw 7.9) are prime examples of area's susceptibility to earthquakes which have affected the spirit of the people of this region. It becomes imperative to carry out seismic hazard assessment which could help people in future.

Different methods have been established to estimate the seismic hazard assessment both in India especially in Himalayan belt and different parts of world using HAZUS, Risk-UE, OPAL and CAPRA models (FEMA, 2003; Daniell, 2011). The results have been very positive. Parvez and Ram (1997) projected PGA for the Indian subcontinent by Eastern United States acceleration attenuation relationship which was between 0.4 to 0.7 g for Himachal Pradesh which is also part of Himalayan belt. Probabilistic approach was used by Parvez and Ram (1999) and Nath and Thingbaijam (2012) for analysis of earthquake hazards in North-East India, the Hindu Kush region and Indian sub-continent and the chances of earthquakes with magnitude greater than 7.0 during a definite interval of time has been predicted on the basis of four probabilistic models, namely, Weibull, Gamma, lognormal and exponential (Chandra et al., 2018) Using statistical models reveals that Kashmir Valley, located in the NW Himalaya have greater possibility to higher magnitude earthquakes, due to its tectono-geomorphic background. Some areas of Kashmir are prone to narrow as well as subduction earthquake (Mridula and Wason, 2014; Nath and Thingbaijam, 2012). Likewise, other studies done around Himalyan belt found the necessity of the determination for booming out susceptibility study to evaluate the populations that are in danger to threat perception of earthquakes, so that suitable extenuation measures can be put in place (Mridula and Wason, 2014). Besides this the Seismic hazard assessment is a useful technique which also helps a great deal in preparation of seismic risk maps and assessment of earthquake protection payments (Masson et al., 2005).

An attempt has been made to assess the probabilistic seismic hazard in the different district headquarters of Kashmir valley within the latitude 33°22' N to 34°43' N and 74° E to 76° E. R crisis software has been used to carry out the analysis in present study. The UHRS curves and contour maps for different return periods have also been prepared. The results of this study can be beneficial in land use development, preparation and extenuation measures that can be taken before another damaging earthquake effects the area. The study holds more importance as the previous studies done did not give the complete details required.

1.1   Study areas

Kashmir is a Neogene Quaternary intermountain basin with distinct NW-SE asymmetric disposition located on the NW portion of the Himalaya Mountains. It was formed as a result of continent-continent collision between the Indian and Eurasian plates. It is bounded by the Zanskar Mountain Range in the ENE and Pir Panjal Range in the WSW. The Kashmir division borders Jammu Division to the south and Ladakh to the east while Line of Control forms its northern and the western border. Southwest of the Pir Panjal Range is a complex pattern of faulting with the super-position of several thrusts, such as the Main Central Thrust (MCT)/Panjal Thrust (PT), MBT/Murree Thrust (MT), Riasi Thrust (RT), and Kotli Thrust (KT). The districts under Kashmir division are Anantnag, Pulwama, Kulgam, Shopian, Srinagar, Budgam, Ganderbal, Baramullah, Kupwara, and Bandipora.

Figure 1 Map of Kashmir Valley and its districts (see online version for colours)

1.2   Sites description

Anantnag, Pulwama, Kulgam, Shopian, Srinagar, Budgam, Ganderbal, Baramullah, Kupwara, and Bandipura districts were used in our study. The study was done between the longitude 74° E to 76° E and the latitude 33°22' N to 34°43' N Cambrian basement rocks of Salkhala Formation are oldest rocks of these areas of Kashmir Valley which have deformed into several isoclinal folds showing high grade of metamorphism. These areas lie on the NW side of the Himalyas comprising of Pir Panal, Zanskar, Karankoram and Ladakh ranges. The MBT underlies the Pir Panjal Range known as Pir Panjal Thrust. Moreover, northern parts of State are heavily faulted making Kashmir valley vulnerable to the earthquakes. Longest strikeslip fault of the Jammu and Kashmir state runs along Zaskar and the Ladakh ranges. According to the Bureau of Indian Standards (IS 1893, 2002), Kashmir Valley falls in the Zone IV and Zone V. According to GSHAP data it lies in the region of high to very high seismic hazard. (Shedlock et al., 2000). Figure 2 shows sites selected and area around radius of 100 km.

Figure 2 Map showing different locations and area surrounding them (see online version for colours)
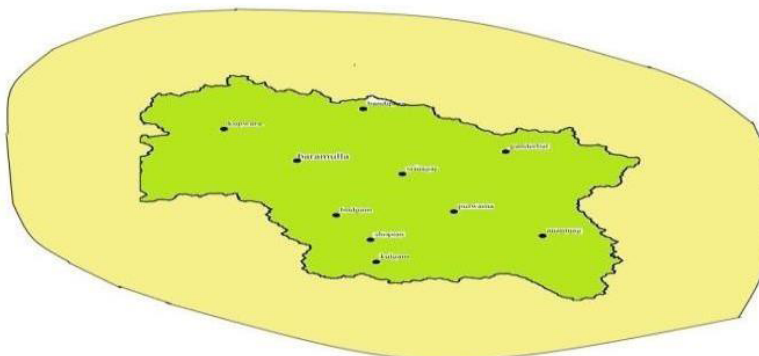
2   Materials and methodology

In this study, the seismic hazard of the Kashmir basin has been evaluated at a 0.1° grid interval covering the region between the longitude 74° E to 76° E and the latitude 33°22' N to 34°43' N using R-CRISIS software version 18.3. A total of 99 tectonic landscapes which include faults were recognised. 32 Seism genic Source Zones (SSZ), were recognised on the basis of seismicity and the tectonics around it. Seismic hazard parameters were then computed for each source zone. Simulation of ground motion for the given soil conditions were done using the ground motions parameters models (GMPM) proposed by Atkinson and Boore (2006). GMPM stands for GMPMs; they use data of detailed ground motions parameters at different positions in the course of different earthquakes to produce equations that are used to guess establish detailed ground motions. These models designate ground motions in relations of median and logarithmic standard deviation. Following steps were involved in this study.

2.1   Classification of seismic sources

The seismic sources were idealised as fault/line sources. In R-CRISIS, line sources are polylines defined by the 3D coordinates of their vertexes It was assumed that the earthquakes occur along a line defined by the source geometry and that the rupture length will be centred at the hypocenter. For each source, values of latitude, longitude and depth are entered. The *K* parameters that define the size of the rupture area can be specified by the user or selected from the various built-in models. For the current study the rupture parameters used are those of Wells and Coppersmith (SRL reverse) (Wells and Coppersmith, 1994) with K1 = .0013804 and K2 = 1.4506. The data regarding various sources is derived from RS, GIS and published sources like Seism genic Atlas of India (SSEISAT, 2005).

2.2   Earthquake catalogue and calculation of seismicity parameters

For calculating the seismic parameters a homogenous earthquake catalogue of all earthquake events converted to single magnitude type – the moment magnitude) was assembled for the region 29°N – 39°N and 70°E – 80°E from the seismic instrumentation network of Indian Meteorological Department (IMD), International Seismological Centre (ISC), US Geological Survey (USGS) (SSEISAT, 2005; Attri and Tyagi, 2010; Clark et al., 1993; Brown et al., 2011) and recurrence model for each seismic source was developed. During this process, the cumulative number of earthquakes of a specified magnitude and greater are obtained, which is normalised over the completeness period to calculate the cumulative frequency. The cumulative frequency (in logarithmic form) is correlated with the specified magnitude, a linear regression analysis is carried out and fitting to the data is performed to obtain the fitted trend equation. This provide estimate of 'a' and 'b' parameter of the G-R model. Equation is used for such purpose

$$\text{Log}_{10}(m) = a - bm \tag{1}$$

- $\lambda(m)$ is the number of earthquakes greater than or equal to magnitude m

- (a, b) values characterise the seismicity of the region.

The threshold magnitude (M_0) was taken as 4. Also the recurrence parameters a, b used in the current study are taken from the study conducted by NDMA (Clark et al., 1993; Brown et al., 2011) for all the 32 Seismogenic zones. The Seism genic zones of interest are the zone 1,6,22 and 28.

The value of mean annual rate of exceedance (λ) of minimum specified, and larger, magnitude earthquakes is obtained from modified G-R relationship 2.

$$\lambda = \exp\left[(\alpha - \beta M_o) \times \left\{\exp - \beta(M - M_o)\right\} - \exp\left\{-\beta(M_{\max} - M_o)\right\}\right]$$
$$\times 1/\left[1 - \exp\left(-\beta(M_{\max} - M_o)\right)\right] \tag{2}$$

where

α $a^{2.303}$

β $b^{2.303}$.

2.3   Attenuation of data

In the present study the GMPM proposed by Atkinson and Boore (2006) has been used to simulate the ground motion for the given soil conditions. Four sets of hazard maps for class C site conditions in terms of the three ground motion parameters, namely, PGA, *Sa* (0.2 *s*) and *Sa* (1.0 *s*) were found out and the uniform hazard response spectrums were constructed for any site located within the study region by IBC (2006) approach by picking the values from the hazard map of that specific site class. The equation (3) is used by PGA/PSA.

$$\log(Y) = c_1 + c_2 M + c_3 M^2 + (c_4 + c_5 M) \times \min\left[\log(R), \log(60)\right]$$
$$+ (c_6 + c_7 M) \times \max\left[\min\left\{\log(R/60), \log(120/60)\right\}, 0\right] \tag{3}$$
$$+ (c_8 + c_9 M) \times \max\left[\log(R/140), 0 + c_{10}R\right]$$

where

$$R = \left(RRUP^2 + C_{11}^2\right) \tag{4}$$

Y = median value of PGA or PSA (g) M is moment magnitude

R_{RUP} is closest distance to the fault-rupture surface (km).

2.4   Spectral coordinates

Exceedance probabilities were computed for the number of intensity levels (spectral coordinates) selected between the lower and upper limit of PGA with either logarithmic or linear (arithmetic) spacing. In our study a total of 15 spectral coordinates were defined for analysis purpose, with values of PGA ranging from 3,000–1,000 cm/s^2 for periods .01 secs to 3 secs, and logarithmic spacing.

2.5   Validation and execution

After inputting all the parameters related to seismicity, attenuation etc. the program was validated for warnings and errors. Once the review of the data validation process was performed by R-CRISIS, the analysis was executed. After the execution, the hazard maps and the disaggregation charts were generated for different time frames, corresponding to different spectral time periods and return periods. These hazard maps generated in R CRISIS were transported to ArcGIS for plotting and mapping.

3   Results and discussions

The results obtained for seismicity hazard parameters and seismic hazard maps and curves are discussed in following sections.

3.1   Seismic hazard parameters

Before finding these parameters delineation of seismic sources and assessment of maximum associated earthquake potential was carried out and major faults and folds were identified in and around the basin likely which are likely to affect it due to occurrence of seismic events on them. Figure 3 shows the identified faults and folds. For analysing Earthquake hazard and preparation of different contour maps, the seismicity hazard parameters like maximum expected magnitude M_{max}, activity rate λ and the a and b value of G-R model are required. These parameters have been found out for each source. The earthquake hazard parameters are shown in Table 1.

Figure 3   Faults (shown in red) and fold (shown in green) map of Jammu and Kashmir (see online version for colours)

Table 1   Seismicity hazard parameters

Source name	Length (km)	M_{max}	Mo	a	b	A	B	λ	COV(β)	No. of magnitudes
BBF	64.313	7.5	4	4.3	0.88	9.9029	2.02664	6.0275	0.092	9
BF	64.06	7.5	4	4.3	0.88	9.9029	2.02664	6.0275	0.092	9
BF1	11.191	6	4	4.3	0.88	9.9029	2.02664	6.0275	0.092	9
BF2	8.272	5.5	4	4.3	0.88	9.9029	2.02664	6.0275	0.092	9
ET	4.977	5	4	4.3	0.88	9.9029	2.02664	6.0275	0.092	9
GCT1	218.56	8	4	4.3	0.91	9.9029	2.09573	4.5721	0.092	9
GCT2	271.36	8	4	4.3	0.91	9.9029	2.09573	4.5721	0.092	9
HFT	77.097	7.5	4	4.3	0.88	9.9029	2.02664	6.0275	0.092	9
JT	147.65	8	4	4.3	0.88	9.9029	2.02664	6.0275	0.092	9
KT1	86.49	7.5	4	4.3	0.88	9.9029	2.02664	6.0275	0.092	9
KT2	29.426	7	4	4.3	0.88	9.9029	2.02664	6.0275	0.092	9
KULBU GH-F	4.865	5	4	4.3	0.88	9.9029	2.02664	6.0275	0.092	9
MBT1	564.84	9	4	4.3	0.88	9.9029	2.02664	6.0275	0.092	9
MBT2	154.74	8	4	4.3	0.88	9.9029	2.02664	6.0275	0.092	9
MBT11	42.537	7	4	4.3	0.88	9.9029	2.02664	6.0275	0.092	9
MBT22	49.612	7	4	4.3	0.88	9.9029	2.02664	6.0275	0.092	9
MBT33	16.225	6.5	4	4.3	0.88	9.9029	2.02664	6.0275	0.092	9
MBT44	15.006	6.5	4	4.3	0.88	9.9029	2.02664	6.0275	0.092	9
MCT	173.92	8	4	4.3	0.88	9.9029	2.02664	6.0275	0.092	9
MCT1	743	9	4	4.3	0.88	9.9029	2.02664	6.0275	0.092	9
MCT2	46.256	7	4	4.3	0.88	9.9029	2.02664	6.0275	0.092	9
MCT3	19.371	6.5	4	4.3	0.88	9.9029	2.02664	6.0275	0.092	9
MKT	253.73	8	4	4.3	0.91	9.9029	2.09573	4.5721	0.092	9
MKT2	90.503	7.5	4	4.3	0.88	9.9029	2.02664	6.0275	0.092	9
MMT	432.22	9	4	4.3	0.88	9.9029	2.02664	6.0275	0.092	9
MT1	3.602	5	4	4.3	0.88	9.9029	2.02664	6.0275	0.092	9
MT2	3.94	5	4	4.3	0.88	9.9029	2.02664	6.0275	0.092	9
MT3	5.196	5.5	4	4.3	0.88	9.9029	2.02664	6.0275	0.092	9
MWT	37.5	7	4	4.3	0.88	9.9029	2.02664	6.0275	0.092	9
OF	10.808	6	4	4.3	0.88	9.9029	2.02664	6.0275	0.092	9
RT	80.256	7.5	4	4.3	0.88	9.9029	2.02664	6.0275	0.092	9
RT1	14.895	6.5	4	4.3	0.88	9.9029	2.02664	6.0275	0.092	9
SRT1	157.73	8	4	4.3	1.01	9.9029	2.32603	1.819	0.092	9
SRT2	56.441	7	4	4.3	1.01	9.9029	2.32603	1.819	0.092	9
SWT	85.288	7.5	4	4.3	0.88	9.9029	2.02664	6.0275	0.092	9
ZT	216.56	8	4	4.3	0.91	9.9029	2.09573	4.5721	0.092	9
F2	34.153	7	4	4.3	1.01	9.9029	2.32603	1.819	0.092	9
F14	84.069	7.5	4	4.3	0.88	9.9029	2.02664	6.0275	0.092	9

Table 1   Seismicity hazard parameters (continued)

Source name	Length (km)	M_{max}	Mo	a	b	A	B	λ	COV(β)	No. of magnitudes
F18	102.11	8	4	4.3	1.01	9.9029	2.32603	1.819	0.092	9
F42	7.002	5.5	4	4.3	1.01	9.9029	2.32603	1.819	0.092	9
F43	13.26	6	4	4.3	1.01	9.9029	2.32603	1.819	0.092	9
F44	10.323	6	4	4.3	1.01	9.9029	2.32603	1.819	0.092	9
F45	10.457	6	4	4.3	1.01	9.9029	2.32603	1.819	0.092	9
F46	36.837	7	4	4.3	1.01	9.9029	2.32603	1.819	0.092	9
F47	37.442	7	4	4.3	0.88	9.9029	2.02664	6.0275	0.092	9
F48	6.54	5.5	4	4.3	0.88	9.9029	2.02664	6.0275	0.092	9
F49	7.228	5.5	4	4.3	0.88	9.9029	2.02664	6.0275	0.092	9
F50	129.08	8	4	4.3	1.01	9.9029	2.32603	1.819	0.092	9
F51	144.67	8	4	4.3	0.88	9.9029	2.02664	6.0275	0.092	9
F52	28.487	6.5	4	4.3	0.91	9.9029	2.09573	4.5721	0.092	9
F53	93.989	7.5	4	4.3	0.88	9.9029	2.02664	6.0275	0.092	9
F54	70.209	7.5	4	4.3	0.88	9.9029	2.02664	6.0275	0.092	9
F55	142.61	8	4	4.3	0.88	9.9029	2.02664	6.0275	0.092	9
F56	9.343	5.5	4	4.3	0.88	9.9029	2.02664	6.0275	0.092	9
F58	6.717	5.5	4	4.3	0.88	9.9029	2.02664	6.0275	0.092	9
F59	20.583	6.5	4	4.3	0.88	9.9029	2.02664	6.0275	0.092	9
F60	29.107	7	4	4.3	0.88	9.9029	2.02664	6.0275	0.092	9
F61	6.005	5.5	4	4.3	0.88	9.9029	2.02664	6.0275	0.092	9
F62	7.105	5.5	4	4.3	0.88	9.9029	2.02664	6.0275	0.092	9
F63	76.662	7.5	4	4.3	0.88	9.9029	2.02664	6.0275	0.092	9
F64	65.738	7.5	4	4.3	0.88	9.9029	2.02664	6.0275	0.092	9
F65	10.579	6	4	4.3	0.88	9.9029	2.02664	6.0275	0.092	9
F66	86.662	7.5	4	4.3	0.88	9.9029	2.02664	6.0275	0.092	9
F67	117.69	8	4	4.3	0.88	9.9029	2.02664	6.0275	0.092	9
F68	110.76	8	4	4.3	0.88	9.9029	2.02664	6.0275	0.092	9
F69	117.69	8	4	4.3	0.88	9.9029	2.02664	6.0275	0.092	9
F70	339.08	8	4	4.3	0.88	9.9029	2.02664	6.0275	0.092	9
F71	22.363	6.5	4	4.3	0.88	9.9029	2.02664	6.0275	0.092	9
F72	201.81	8	4	4.3	0.88	9.9029	2.02664	6.0275	0.092	9
F74	545.94	9	4	4.3	1.01	9.9029	2.32603	1.819	0.092	9
F75	23.302	6.5	4	4.3	0.88	9.9029	2.02664	6.0275	0.092	9
F75-1	250.32	8	4	4.3	0.88	9.9029	2.02664	6.0275	0.092	9
F76	154.61	8	4	4.3	0.81	9.9029	1.86543	11.486	0.092	9
F77	296.35	8	4	4.3	0.81	9.9029	1.86543	11.486	0.092	9
F78	50.466	7	4	4.3	0.81	9.9029	1.86543	11.486	0.092	9
F79	92.53	7.5	4	4.3	0.81	9.9029	1.86543	11.486	0.092	9

Table 1 Seismicity hazard parameters (continued)

Source name	Length (km)	M_{max}	Mo	a	b	A	B	λ	COV(β)	No. of magnitudes
F80	98.162	7.5	4	4.3	0.81	9.9029	1.86543	11.486	0.092	9
F81	30.467	7	4	4.3	0.81	9.9029	1.86543	11.486	0.092	9
F82	191.22	8	4	4.3	0.81	9.9029	1.86543	11.486	0.092	9
F83	167.48	9	4	4.3	0.81	9.9029	1.86543	11.486	0.092	9
F84	209.86	8	4	4.3	0.81	9.9029	1.86543	11.486	0.092	9
F85	47.558	7	4	4.3	0.88	9.9029	2.02664	6.0275	0.092	9
F86	15.356	6.5	4	4.3	0.88	9.9029	2.02664	6.0275	0.092	9
F87	41.319	7	4	4.3	0.88	9.9029	2.02664	6.0275	0.092	9
F88	73.789	7.5	4	4.3	0.88	9.9029	2.02664	6.0275	0.092	9
F89	29.639	7	4	4.3	0.91	9.9029	2.09573	4.5721	0.092	9
F90	7.772	5.5	4	4.3	0.91	9.9029	2.09573	4.5721	0.092	9
F91	54.129	7	4	4.3	0.91	9.9029	2.09573	4.5721	0.092	9
FOLD1	4.681	5	4	4.3	0.88	9.9029	2.02664	6.0275	0.092	9
FOLD2	78.557	7.5	4	4.3	0.88	9.9029	2.02664	6.0275	0.092	9
FOLD3	65.545	7.5	4	4.3	0.88	9.9029	2.02664	6.0275	0.092	9
FOLD4	182.84	8	4	4.3	0.88	9.9029	2.02664	6.0275	0.092	9
FOLD5	73.177	7.5	4	4.3	0.88	9.9029	2.02664	6.0275	0.092	9
FOLD6	93.395	7.5	4	4.3	0.88	9.9029	2.02664	6.0275	0.092	9
FOLD7	40.989	7	4	4.3	0.88	9.9029	2.02664	6.0275	0.092	9
FOLD8	23.121	6.5	4	4.3	0.88	9.9029	2.02664	6.0275	0.092	9
FOLD9	24.033	6.5	4	4.3	0.88	9.9029	2.02664	6.0275	0.092	9
FOLD10	24.953	6.5	4	0	0.88	9.9029	2.02664	6.0275	0.092	9
FOLD11	49.433	7	4	4.3	0.88	9.9029	2.02664	6.0275	0.092	9

3.2 Seismic hazard maps and ground motion parameters

Four sets of hazard maps for class C site conditions according to (Atkinson and Boore, 2006) in terms of the three ground motion parameters, namely, PGA, *Sa* (0.2 *s*) and *Sa* (1.0 *s*) were found out.

The PGA values for the return period of 500 years were ranging from 372 cm/s^2 (.38 g) for moderate case of earthquake to 2,451 cm/s^2 (2.5 g) for the worst possible case of earthquake. Due to site amplification, the values reported in this study were on the higher side as compare the values reported by NDMA (Brown et al., 2011) for the same return period where PGA values presented for class A sites was ranging from 50–118 cm/s^2 (0.05–0.12 g). The values obtained in this study were also higher than those reported by Zafarani et al. (2017) obtained by a deterministic approach (design ground acceleration ranges from 79–148 cm/s^2). When compared with the case 1 (varying *b* value) estimates of Parvez et al. (2003) and Patil et al. (2014) that range between 75–148 g, it can be seen that their values underestimates the hazard in this region. Hence, consideration of the fault level seismicity is found to map the seismic hazard more realistically. IS 1893 (2002) designates some parts of the valley as Zone V (very severe) and some as Zone IV (severe) with zero period acceleration values as 0.36 and 0.24 g,

respectively, for maximum considered earthquake (MCE) scenario. However, on comparison with the PGA values at different sites with 2,500-year return period, it can be seen that values estimated are in the ranges of 600 cm/s^2 (0.62 g) for moderate earthquake to 2,940 cm/s^2 (3 g) for the worst possible combination of earthquake magnitude and the site. Similarly, the hazard levels are underestimated for the areas depicted as zone IV. Hence, using these hazard curves, it is possible to extract the response spectrums for design basis earthquake and MCE which correspond to 2% probability of exceedance (considered in this study) during the design life of 50 years (Clark et al., 1993). The resulting response spectra are known as uniform hazard response spectrum (UHRS) due to the assumption of uniform probability of exceedance throughout the frequency ranges.

The UHRS curves for various district headquarters are shown for four return periods of 50,100, 500, 2,500 years respectively in Figures 16, 17, 18, and 19 respectively. The contour plots of short period *Sa* (0.2 *s*) and long period *Sa* (1.0 *s*) spectral accelerations have been estimated in addition to PGA contours (Figures 4–15) for conducting dynamic analysis in tall or irregular structures showing complex behaviour, as against simple structures where PGA is sufficient for analysis by equivalent static method. From the PGA values for different return periods, the districts of Kupwara, Baramulla, Budgam, Shopian and parts of Pulwama and Kulgam exhibit higher hazard levels than the districts of Ganderbal, Anantnag, Bandipora, Srinagar and major parts of Kulgam district. Most importantly, the seismic hazard of the region surrounding Shopian, Budgam and Baramulla are found to be the highest within the study region.

Figure 4   PGA contours with a return period of 50 years (see online version for colours)
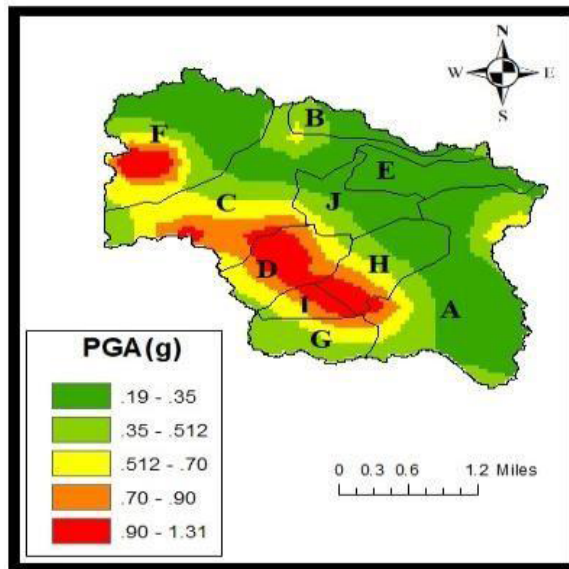
Figure 5 PGA contours with a return period of 100 years (see online version for colours)
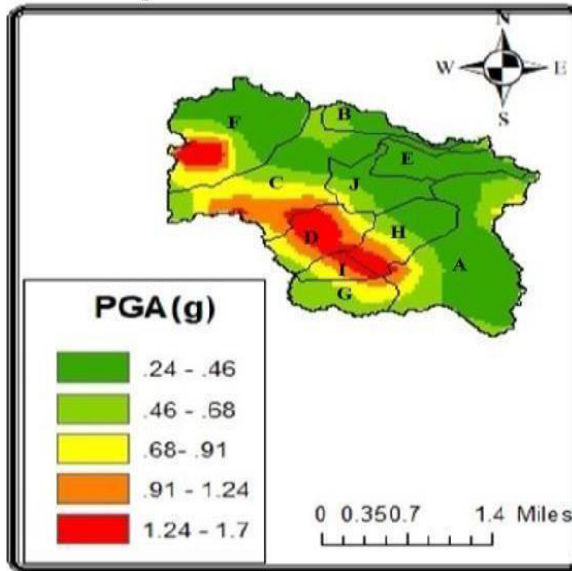
Figure 6 PGA contours with a return period of 500 years (see online version for colours)
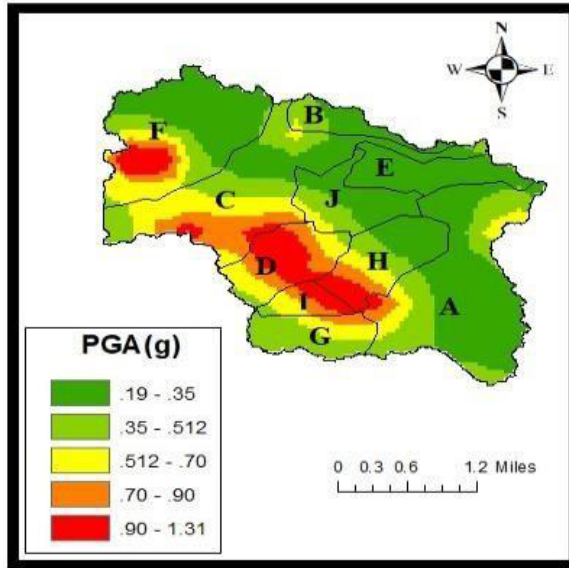
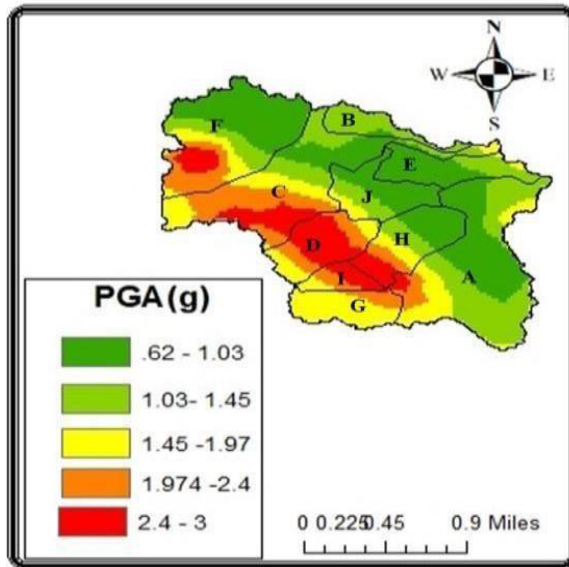**Figure 7**   PGA contours with a return period of 2,500 years (see online version for colours)

Figure 8   *Sa* (0.2 s) contours with a return period of 50 years (see online version for colours)
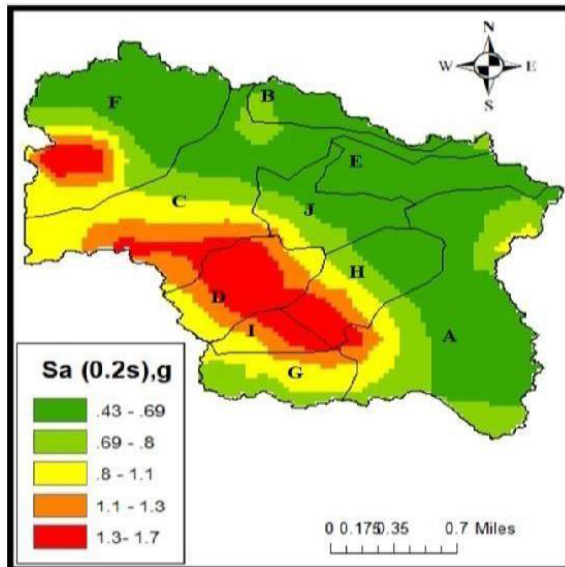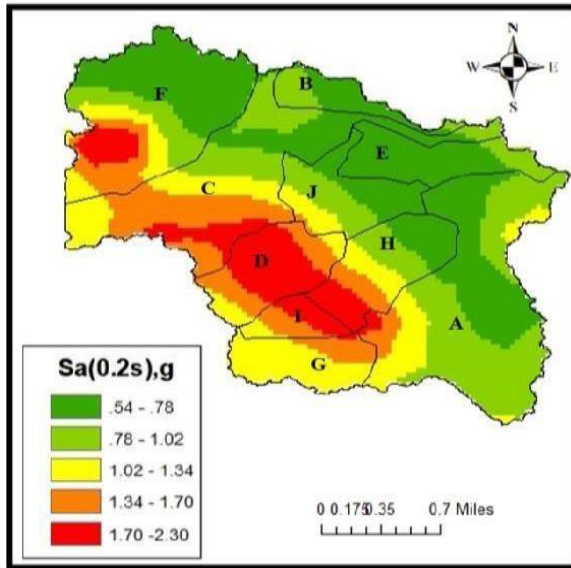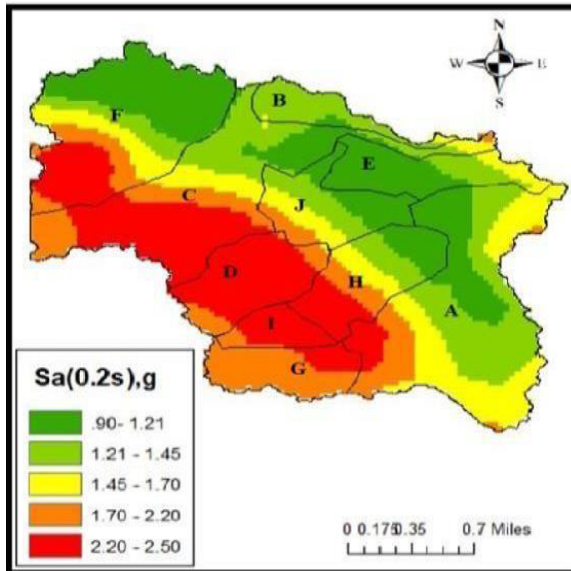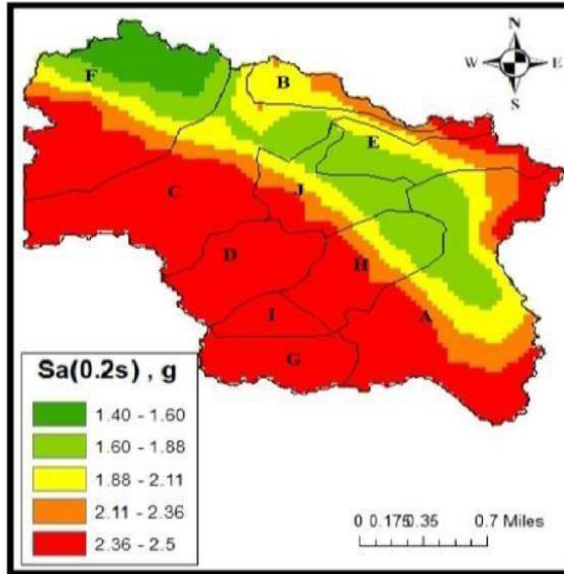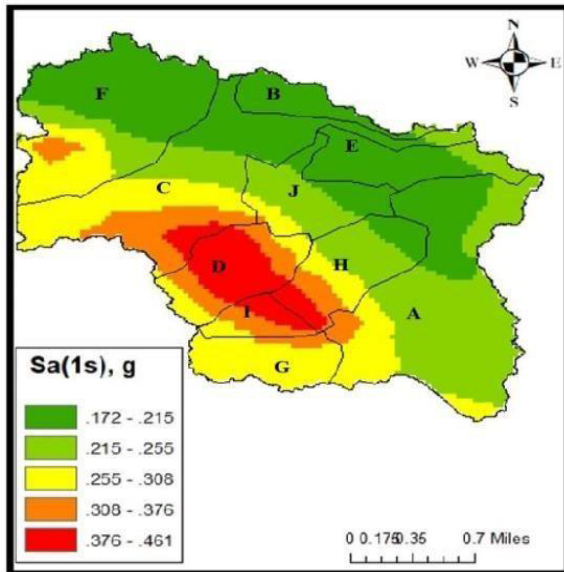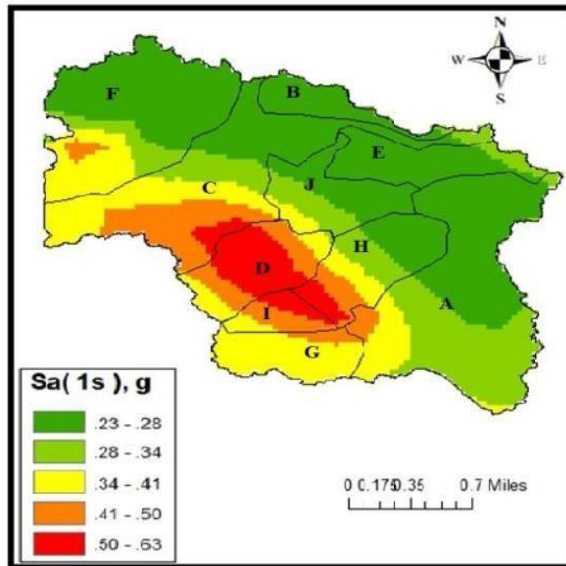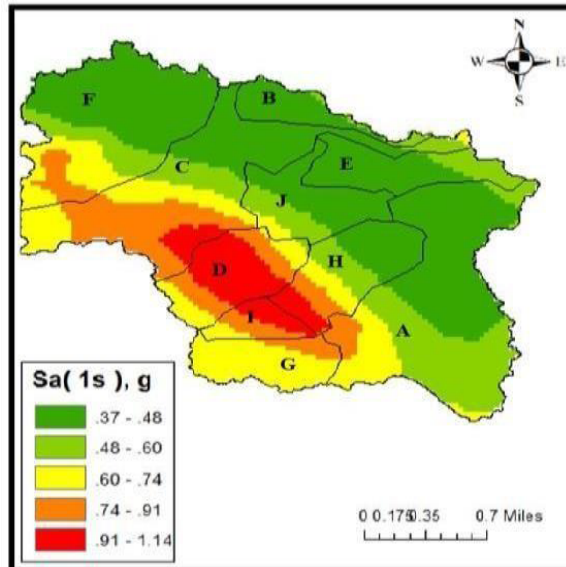
Figure 9 *Sa* (0.2 *s*) contours for a return period of 100 years (see online version for colours)

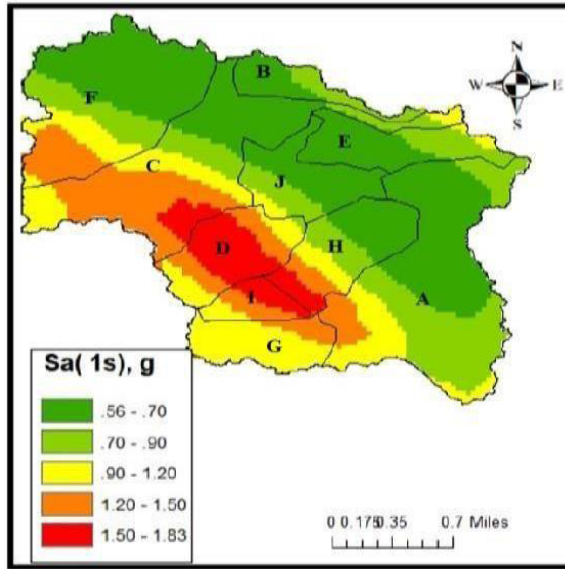**Figure 10** *Sa* (0.2 *s*) contours for a return period of 500 years (see online version for colours)

Figure 11   *Sa* (0.2 *s*) contours with a return period of 2,500 years (see online version for colours)

Figure 12   *Sa* (1 *s*) contours for a return period of 50 years (see online version for colours)
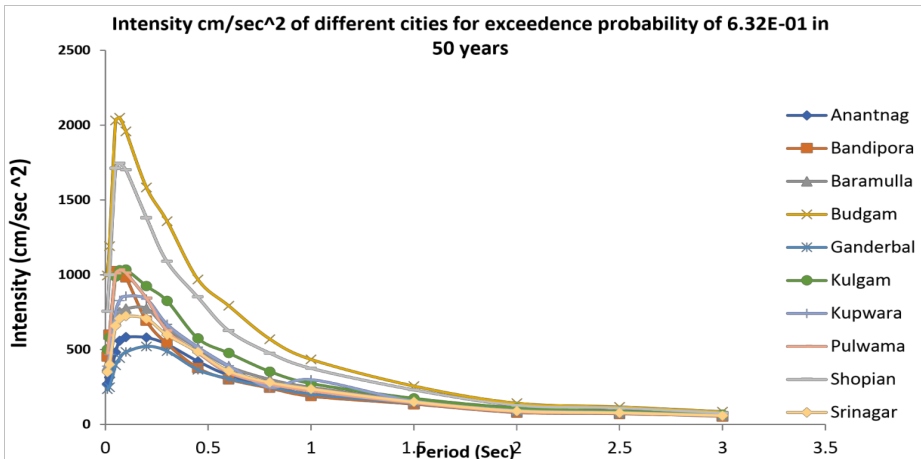
Figure 13 *Sa* (1 *s*) contours for a return period of 100 years (see online version for colours)

Figure 14 *Sa* (1 *s*) contours for a return period of 500 years (see online version for colours)

Figure 15   *Sa* (1 *s*) contours for a return period of 2,500 years (see online version for colours)

Where A is Anantnag, B is Bandipora, C is Baramulla, D is Bugdam, E is Ganderbal, F is Kupwara, G is Kulgam, H is Pulwama, I is Shopian and J is Srinagar.

Figure 16   UHRS curves for return period of 50 years (see online version for colours)

Figure 17 UHRS curves for a return period of 100 years (see online version for colours)
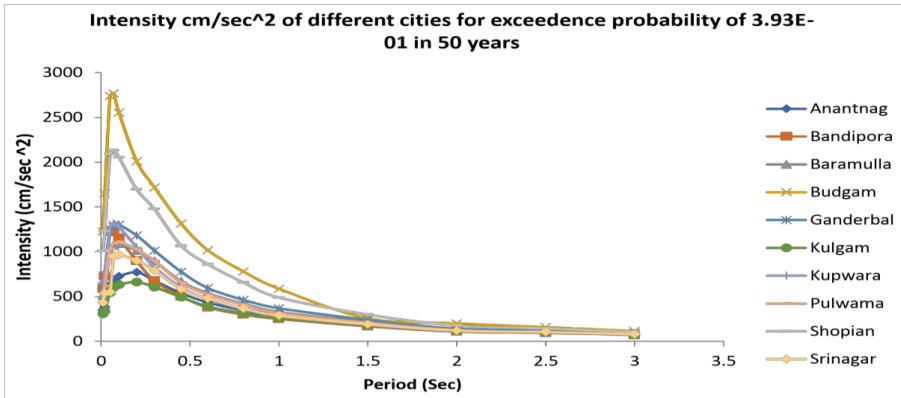

Figure 18 UHRS curves for a return period of 500 years (see online version for colours)
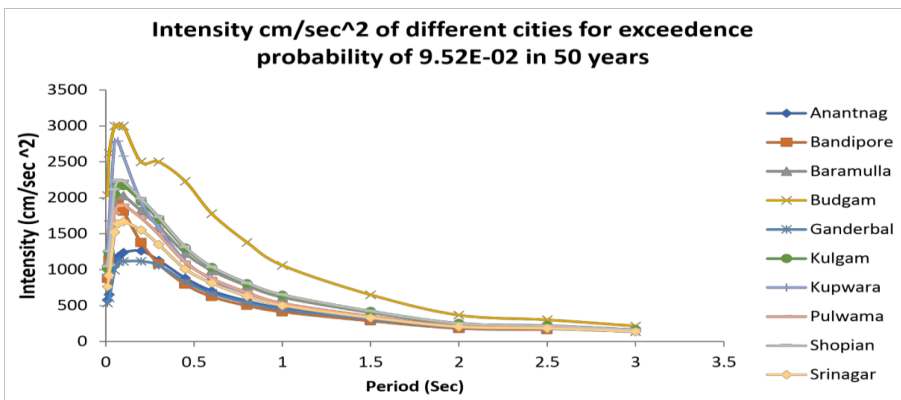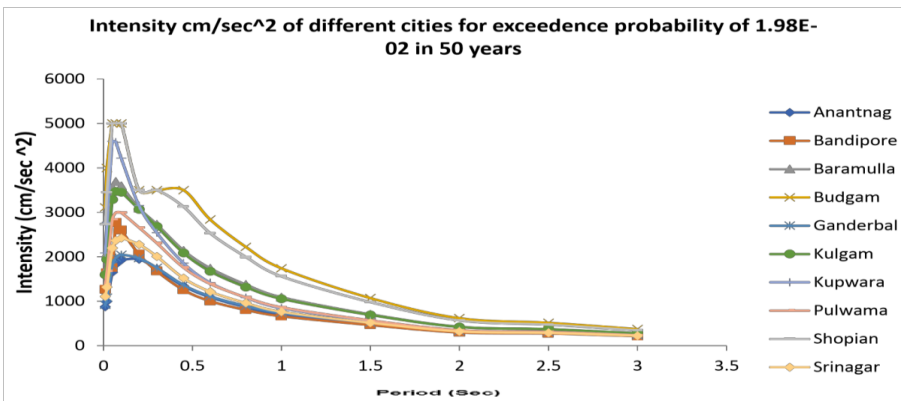

Figure 19 UHRS curves for return period of 2,500 years (see online version for colours)

4   Conclusions

From these seismic hazard curves, the site-specific uniform hazard response spectra for the districts have been presented for 50, 100, 500- and 2,500-year return periods. Also, the contour maps of three ground motion parameters, namely, peak ground acceleration (PGA), short period *Sa* (0.02 *s*) and long period *Sa* (1.0 *s*) spectral acceleration for return periods 50, 100, 500, 2,500 years, are presented for this region. In this study it was found that the PGA values for the return period of 500 years were ranging from 372 cm/s^2 (.38g) for moderate case of earthquake to 2,451 cm/s^2 (2.5 g) for the worst possible case of earthquake. However, on comparison with the PGA values at different sites with 2,500-year return period, it was found that values estimated are in the ranges of 600 cm/s^2 (0.62 g) for moderate earthquake to 2,940 cm/ s^2 (3 g) for the worst possible combination of earthquake magnitude and the site. The comparison of the present estimates with the earlier studies done by Parvez et al. (2003) and Patil et al. (2014) highlights the need to consider the local site variability in the hazard computation. Also, the regions surrounding the city of Shopian, Budgam, Baramulla and Kupawara were found to have much higher seismic hazard levels than previously reported. The estimated hazard values for these regions highlight that the zonal spectral values are underestimated in the Indian Codal Provisions. Hence, the maps developed in this study using a detailed probabilistic framework can be used for assessing the seismic vulnerability of the existing structures. The obtained hazard curves combined with UHRS can be used to construct risk maps for the region. Also, there is a need for estimating the seismic hazard of this region in terms of other ground motion parameters such as spectral velocity, spectral displacements., which are necessary for the performance-based design of structures.

References

Ambraseys, N. and Bilham, R. (2000) 'A note on the Kangra M s = 7.8 earthquake of 4 April 1905', *Current Science*, Vol. 79, No. 1, pp.45–50.

Atkinson, G.M. and Boore, D.M. (2006) 'Earthquake ground-motion prediction equations for eastern North America', *Bulletin of the Seismological Society of America*, Vol. 96, No. 6, pp.2181–2205.

Attri, S.D. and Tyagi, A. (2010) *Climate Profile of India*, Environment Monitoring and Research Center, India Meteorology Department: New Delhi, India.

Baker, J.W. (2008) *An Introduction to Probabilistic Seismic Hazard Analysis (PSHA)*, White Paper, Version 1.3.

Banerjee, P. and Bürgmann, R. (2002) 'Convergence across the northwest Himalaya from GPS measurements', *Geophysical Research Letters*, Vol. 29, No. 13, pp.30–31.

Brown, P., Zhu, M., Wu, Q. and Lu, X. (2011) 'Network-aware data movement advisor', *Proceedings of the First International Workshop on Network-Aware Data Management*, ACM, pp.31–40.

Chandra, R., Dar, J.A., Romshoo, S.A., Rashid, I., Parvez, I.A., Mir, S.A. and Fayaz, M. (2018) 'Seismic hazard and probability assessment of Kashmir valley, northwest Himalaya, India', *Natural Hazards*, Vol. 94, No. 3, pp.1451–1477.

Clark, R.N., Swayze, G.A., King, T.V., Gallagher, A.J. and Calvin, W.M. (1993) *The US Geological Survey, Digital Spectral Reflectance Library: Version 1: 0.2 to 3.0 Microns*.

Daniell, J.E. (2011) 'Open source procedure for assessment of loss using global earthquake modelling software (OPAL)', *Natural Hazards and Earth System Sciences*, Vol. 11, No. 7, pp.1885–1899.

Federal Emergency Management Agency (FEMA) (2003) *HAZUS-MH Technical Manual*, Washington DC, USA.

IBC, I. (2006) *International Building Code*, International Code Council, Inc. (formerly BOCA, ICBO and SBCCI), Vol. 4051, pp.60478–5795.

IS 1893 (2002) *Criteria for Earthquake Resistant Design of Structures – Part 1: General Provisions and Buildings*, Standard Publishers, New Delhi, India

Kaneda, H., Nakata, T., Tsutsumi, H., Kondo, H., Sugito, N., Awata, Y. and Yeats, R.S. (2008) 'Surface rupture of the 2005 Kashmir, Pakistan, earthquake and its active tectonic implications', *Bulletin of the Seismological Society of America*, Vol. 98, No. 2, pp.521–557.

Malik, J.N. and Mohanty, C. (2007) 'Active tectonic influence on the evolution of drainage and landscape: geomorphic signatures from frontal and hinterland areas along the Northwestern Himalaya, India', *Journal of Asian Earth Sciences*, Vol. 29, Nos. 5–6, pp.604–618.

Masson, F., Chéry, J., Hatzfeld, D., Martinod, J., Vernant, P., Tavakoli, F. and Ghafory-Ashtiani, M. (2005) 'Seismic versus aseismic deformation in Iran inferred from earthquakes and geodetic data', *Geophysical Journal International*, Vol. 160, No. 1, pp.217–226.

Mitra, S., Paul, H., Kumar, A., Singh, S.K., Dey, S. and Powali, D. (2015) 'The 25 April 2015 Nepal earthquake and its aftershocks', *Current Science*, Vol. 108, No. 10, pp.1938–1943.

Mridula, S.A. and Wason, H.R. (2014) 'Probabilistic seismic hazard assessment in the vicinity of MBT and MCT in western Himalaya. Research Inventy', *Int. J. Eng. Sci.*, Vol. 4, No. 11, pp.21–34.

Nakata, T. (1989) 'Active faults of the Himalaya of India and Nepal', *Geological Society of America Special Paper*, Vol. 232, No. 1, pp.243–264.

Nath, S.K. and Thingbaijam, K.K.S. (2012) 'Probabilistic seismic hazard assessment of India', *Seismological Research Letters*, Vol. 83, No. 1, pp.135–149.

Parvez, I.A. and Ram, A.V.A.D.H. (1997) 'Probabilistic assessment of earthquake hazards in the north-east Indian peninsula and Hindukush regions', *Pure and Applied Geophysics*, Vol. 149, No. 4, pp.731–746.

Parvez, I.A. and Ram, A.V.A.D.H. (1999) 'Probabilistic assessment of earthquake hazards in the Indian subcontinent', *Pure and Applied Geophysics*, Vol. 154, No. 1, pp.23–40.

Parvez, I.A., Vaccari, F. and Panza, G.F. (2003) 'A deterministic seismic hazard map of India and adjacent areas', *Geophysical Journal International*, Vol. 155, No. 2, pp.489–508.

Patil, N.S., Das, J., Kumar, A., Rout, M.M. and Das, R. (2014) 'Probabilistic seismic hazard assessment of Himachal Pradesh and adjoining regions', *Journal of Earth System Science*, Vol. 123, No. 1, pp.49–62.

Rajendran, C.P., John, B. and Rajendran, K. (2015) 'Medieval pulse of great earthquakes in the central Himalaya: viewing past activities on the frontal thrust', *Journal of Geophysical Research: Solid Earth*, Vol. 120, No. 3, pp.1623–1641.

Shedlock, K.M., Giardini, D., Grunthal, G. and Zhang, P. (2000) 'The GSHAP global seismic hazard map', *Seismological Research Letters*, Vol. 71, No. 6, pp.679–686.

SSEISAT (2005) *Seismotectonic Atlas of India*, Geological Survey of India.

Valdiya, K.S. (1980) 'The two intracrustal boundary thrusts of the Himalaya', *Tectonophysics*, Vol. 66, No. 4, pp.323–348.

Wells, D.L. and Coppersmith, K.J. (1994) 'New empirical relationships among magnitude, rupture length, rupture width, rupture area, and surface displacement', *Bulletin of the Seismological Society of America*, Vol. 84, No. 4, pp.974–1002.

Zafarani, H., Hajimohammadi, B. and Jalalalhosseini, S.M. (2017) 'Earthquake hazard in the Tehran region based on the characteristic earthquake model', *Journal of Earthquake Engineering*, Vol. 23, No. 9, pp.1–27.